Analysis of Protein–Protein Interaction by Simulation of Small-Zone Size-Exclusion Chromatography: Application to an Antibody–Antigen Association†

Fred J. Stevens
Division of Biological and Medical Research, Argonne National Laboratory, Argonne, Illinois 60439
Received June 24, 1985

ABSTRACT: The association of two or more macromolecules results in the formation of a complex characterized by a larger Stokes radius than that of its components. Therefore, analytical procedures such as ultracentrifugation and size-exclusion gel chromatography that resolve molecules on the basis of size have been used to characterize the association. In this paper we describe an iterative computer simulation of small-zone size-exclusion gel filtration. The simulation describes univalent and bivalent interactions of proteins of equal and nonequal molecular weight and appears to have both qualitative and quantitative application to the evaluation of protein–protein interaction as revealed by alteration of chromatographic elution profiles. To test the validity of the simulation, the model was applied to an antibody–antigen interaction by determining the association constant (K_a) for the interaction between the binding fragment derived from a human immunoglobulin A rheumatoid factor and the antigenic fragment obtained from a human myeloma immunoglobulin G. The self-consistency of the estimated K_a values obtained with a valence value of 2 in contrast to the lack of self-consistency if an antigenic valence of 1 was assumed was taken to support the ability of the algorithm to reasonably emulate the chromatographic processes of interacting proteins. In conjunction with the computer simulation, a sensitive microcomputer-interfaced chromatography system was assembled, which is capable of analyzing 300 ng of protein in less than 1 h. This combination of rapid reagent-conservative chromatography and simulation analysis may contribute to the usefulness of small-zone gel filtration in studies of protein–protein interaction.

The association of two polypeptide macromolecules to form a complex provides a basis for analyses of the interaction by size-exclusion gel filtration, in which the characteristic elution behavior of a molecule is, in principle, primarily determined by its hydrodynamic volume or Stokes radius [for review, see Ackers (1975)]. A common strategy in chromatographic studies has been based on the introduction of a large-zone sample to the column. In these experiments, the volume applied to the column is a significant portion of the total column volume, leading to the formation of a concentration plateau within which no dilution of sample occurs. The elution rate of this plateau is determined by an average molecular weight of the free and complexed polypeptide species present. This estimate of the average molecular weight is used to calculate a value for the association constant (K_a)[1] governing the equilibrium ratio between complex and free species.

The large-zone technique was further advanced by Ackers and co-workers, who analyzed the information inherent in the shapes of the leading and trailing edges of the large zone (Ackers & Thompson, 1965; Zimmerman & Ackers, 1971; Zimmerman et al., 1971). Numerical solution of the solute continuity equation enabled interpretation of the relationship between the shape of these boundaries and the polymerization-dependent dispersion of the solute during development of the column run. In addition to the influence of the association constant and reaction stoichiometry, the contribution of the reaction rate constants was investigated by Zimmerman (1974).

Large-zone chromatography has the potential to require relatively large quantities of solute. However, since a mathematical analysis of the elution characteristics of a small-zone mixture of interacting components has not proven tractable, small-zone chromatography has been limited to qualitative study or description of protein interactions, often to verify the presence of association–dissociation phenomena (Andrews, 1964; Sullivan & Riggs, 1967; Dickerman et al., 1981). The difficulty of a mathematical description of the interactive small-zone elution process results from the fact that the equilibrated composition of the sample at any point on the column is a direct function of the concentrations of the species present at that point. These concentrations are dependent upon column dimensions and the characteristics that govern the development of the column: solvent flow rate, solute elution rate, and diffusion rates. As clearly defined by Zimmerman and Ackers (1971), the elution position of a self-associating protein cannot be equated with the position attained by a protein of molecular weight equal to the average molecular weight of the applied mixture.

Two special applications of small-zone gel filtration have been described. The Hummel and Dreyer (1962) method was developed to quantify the binding of a ligand to a macromolecule by examining the chromatographic behavior of a mixture of protein and ligand on a column equilibrated with ligand. A simulation of Hummel–Dreyer chromatography was developed by Cann and Hinman (1976). Recently, Endo and co-workers (Endo et al., 1982; Endo & Wada, 1983) have developed a procedure they refer to as affinity chromatography without immobilized ligands or zone-interference chromatography. The method is based on the displacement in the

† This work was supported by the U.S. Department of Energy under Contract W-31-109-ENG-38 and by U.S. Public Health Service Research Grant CA10056.

[1] Abbreviations: Ig, immunoglobulin; Fab, Ig antigen binding fragment; Fc, Ig "crystallizable" fragment; RF, rheumatoid factor; RL, run length; CL, column length; ADC, analog to digital converter; K_a, association constant.

0006-2960/86/0425-0981$01.50/0

elution position on a gel permeation column of a slowly migrating zone of reactant resulting from interaction with another, more rapidly migrating, component applied as a second sequential sample to the column. Under conditions in which the more rapidly eluting component is present in sufficient excess to result in a pseudo-first-order relationship between the two reactants, the authors have derived a relationship expressing the displacement of the elution position (volume) as the product of the K_a and the quantity of the more rapidly eluting component applied.

Another quantitative approach to analysis of complex formation during small-zone size-exclusion gel filtration (Stevens et al., 1980; Stevens & Schiffer, 1981) characterized the elution behavior of self-associating antibody light chains by means of an iterative simulation rather than by a definitive mathematical description of the chromatographic process. Conceptually, this approach was similar to that formulated by Cox (1965a,b, 1978) and others (Cann & Goad, 1965; Dishon et al., 1966; Kegeles & Cann, 1978) to describe the transport properties of self-associating or mixed-associating systems (Cann, 1982) during electrophoresis or ultracentrifugation. This simulation of interactive chromatography provided qualitative interpretation of the shapes and positions exhibited by several of the immunoglobulin light chains (Stevens et al., 1980); potential quantitative merit was suggested by the correspondence of the K_a value assigned to one of these Bence–Jones proteins, Au, with the value determined in another laboratory by detailed spectroscopic analysis of the self-association of the molecule (Maeda et al., 1978). In this paper, further development of the iterative simulation is described. The algorithm has been redesigned to model mixed associations and the possibility of bivalent association. Additionally, a data acquisition system has been developed that provides direct quantitative comparison of experimentally obtained data and simulated data.[2]

Materials and Methods

RF Preparation. Plasma containing an IgA rheumatoid factor (RF) designated SCH (Kosaka & Solomon, 1980) was obtained from Dr. A. Solomon (University of Tennessee, Knoxville, TN). Defibrinated plasma was passed through a 5 × 140 cm column of AcA22 (LKB) in 0.16 M borate, 0.13 M NaCl, and 0.05 M ϵ-aminocaproic acid, pH 8. Fractions containing a mixture of IgA and IgG were further purified by passage through a column of Protein A–Sepharose CL-4B to absorb the IgG. Finally, the IgA was rechromatographed on AcA22 to separate polymeric and monomeric IgA.

Fab was prepared from SCH by Dr. W. C. Hanly (University of Illinois at Chicago). The purified RF was incubated with an IgA-specific gonococcal protease (Plaut et al., 1977) obtained from Dr. A. G. Plaut (Tufts-New England Medical Center, Boston, MA). The resulting Fab_α and Fc_α fragments were separated on a 2.5 × 150 cm column of Sephadex G-200 in the borate-buffered saline. The Fab pool was rechromatographed on Sephadex G-100.

Fc Preparation. Serum containing a human myeloma immunoglobulin was obtained from Dr. W. C. Hanly. The Ig, designated DRI, was classified as an IgG_1 by use of isotypically specific antisera. The IgG was purified by ammonium sulfate precipitation and gel filtration. The Fc fragment was prepared by digestion with papain (Worthington) at 37 °C for 18 h. Cysteine-activated papain was added to 1 mL of antibody solution containing 9–10 mg of IgG to a final ratio of approximately 1:50 (w/w). Fc was separated from other proteolytic fragments and undigested material by adsorption with Protein A–Sepharose followed by chromatography on Sephadex G-75.

F-6, T-15. $F(ab')_2$ fragments, prepared from the murine Igs T-15 and F-6, were obtained from Dr. H. Kohler (Roswell Park, Rochester, NY). The T-15 protein is a plasmacytoma-produced IgA that binds phosphorylcholine; F-6 is synthesized by a hybridoma cell line selected for specificity against idiotypic determinants of T-15. The $F(ab')_2$ fragments were reduced and alkylated to form monomeric F(ab'). The dimer interchain disulfide bonds were reduced by incubation of protein (5.3 mg/mL) with 0.25 mM dithiothreitol. After incubation for 1 h, iodoacetamide was added to a final concentration of 0.5 mM. An additional incubation of at least 1 h was followed by application to a column of Bio-Gel P-100 (400 mesh). Fractions of 0.1 mL were collected.

Chromatography System. A glass column (2 mm i.d.) was packed with Superose-12 (Pharmacia, Piscataway, NJ) to a bed height of approximately 70 cm. One of two syringe pump components of the Pharmacia FPLC system was used to drive the buffer (0.1 M phosphate, pH 7.0, 0.15 M NaCl) at a flow rate of 2.0 mL/h. The syringe was returned to a defined reference point for initialization prior to each run to assure uniformity of volume delivery. A multiposition valve (V-7, Pharmacia) was used for sample injection (20 μL); the sample loop remained in-line during the full development of the run (1 h). Antibody–antigen mixtures were incubated for 2 h prior to injection.

Column effluent was monitored at 280 nm. The flow cell (Pharmacia HR-10) had a path length of 10 mm and an illuminated volume of 8.7 μL. The output voltage of the detector (100 mV) was amplified 10-fold and subsequently digitized by a 12-bit analog to digital converter (ADC) on a ADALAB interface card (Interactive Microware, Inc., State College, PA). The interface operates with an Apple 2/e microcomputer. Data were stored on magnetic disk prior to transfer to a PDP 11/44 minicomputer.

An operating program was written in Applesoft BASIC and uses the QUICK I/O interface operating language provided by Interactive Microware, Inc. The program interacts with the operator to set up and document the chromatographic run. The system collected 1000 data points per run with each point the average of 10 readings from the ADC. The data set and the documentation of the run were both written to disk for later use. The elution profile is displayed on the Apple monitor during the development of the chromatogram. Both the plot of collected data and a listing of the documentation are provided at the completion of the run.

Data were transferred by telephone from the Apple 2/e microcomputer to a PDP 11/44. The file-transfer capability was provided by the KERMIT terminal emulator program developed at Columbia University. A program was written for the 11/44 to convert the collected data from the ADC format to absorbance values; each point was multiplied by the full scale (AUFS) value of the monitor during the run and divided by 2047, the maximum output of a 12-bit ADC. An option was provided to zero the chromatogram base line to facilitate comparison and manipulation of data sets. An appropriate base-line segment was designated; the average absorbance value of this segment was subtracted from all values collected during the course of the run. To simplify correlation with data created by the chromatography simulation, the number of points describing the elution profile was reduced to 250, the

[2] A preliminary report of this work has been presented (Stevens & Ainsworth, 1985).

arbitrary number of points obtained for a complete simulated run. The rescaled data were written to a file for routine use; the original data were retained for future analyses.

The 11/44 was also host for the simulation written in DEC BASIC. Development of a Fortran 77 version suitable for the PDP 11/44 and IBM/370 is in progress. The 11/44 was used to directly compare experimental data and simulated data calculated by means of the algorithm outlined below.

Simulation. No assumptions were made about the mechanism of size-exclusion gel filtration; specifically, no partitioning formulation between mobile and stationary phases was attempted. The simulation was not designed to model the process of gel filtration but rather the consequences. The model is, therefore, derived from the premise that a numerical procedure that satisfactorily describes the time-dependent distribution of solutes during the development of the column will also describe the elution behavior consequences of interaction between the solutes.

The algorithm was based on a visualization of the chromatography column as a linear array of cells of equal volume. Although this is analogous to a "theoretical plate" formulation, the similarity was not intended. Cox (1965a,b, 1969, 1978) described the cell in the ultracentrifugation as an array of boxes. His compartments were of varying sizes, however, to avoid an anomalous distortion of the simulated boundary due to numerical dispersion [for discussion, see Cox (1978)].

Scaling of the algorithm parameters in the example discussed in this paper was accomplished by defining 250 algorithm cycles as the total run length (RL) and defining 10 μL as the cell volume. As a result, a typical 20-μL sample occupied cells 1 and 2 at the initiation of the simulation. The elution rate of a "totally included" reference molecule such as acetone was taken as the unitary velocity, thus fixing the column length (CL) by reference to the elution time observed for acetone or an equivalent molecule.

One iteration cycle of the algorithm comprises five steps. An equilibration calculation (step 1) to determine the free and complexed composition of each cell is followed by a translation step (step 2). The translation step emulates the migration of the protein through the column on the basis of the velocities of the components and their respective dispersion characteristics. Translation is followed by another equilibration (step 3) prior to the execution of a diffusion step (step 4). Diffusion, in addition to dispersion, accounts for band spreading. As the influence of diffusion depends on the concentration gradient, this effect is most prominent early in the run. Step 5 monitors and records the concentration (absorbance) at the detector position. Reequilibration of the cell contents reinitiates the cycle.

Three parameters—velocity, diffusion, and dispersion—characterize the migration behavior of an individual protein through the column. The velocity parameter is determined by the time elapsed between injection of the sample and the elution of the sample peak. The diffusion and dispersion parameters together determine the peak width at elution and the kinetics of sample dilution during the column run. The diffusion parameter is, in principle, equivalent to the standard definition of a diffusion coefficient for a molecule in that it defines the time dependence of the spreading of a solute band. However, the numerical value of the simulation parameter is not equal to a physical value. The diffusion parameter is not flow rate dependent.

The dispersion parameter, on the other hand, is related to the flow rate. Whereas the velocity parameter represents the center of mass displacement of the molecules in a given cell during each cycle of the algorithm, the dispersion parameter represents the Gaussian spread about this mean position. The spread is expected to be minimized under conditions in which equlibration between mobile and stationary phases is complete; hence, the dispersion parameter is velocity-dependent, increasing with the flow rate of the mobile phase or the linear velocity of the solute. The minimum value of the dispersion parameter also implicitly includes a flow rate independent contribution accounting for band spreading due to packing irregularities in the column. The relationship of the dispersion parameter and the intrinsic numerical dispersion noted above will be examined later.

Translation Routine. The previous algorithm (Stevens & Schiffer, 1981) was limited in its application to a description of the chromatographic characteristics of self-associating proteins. As only two elution velocities were needed in this circumstance, it was satisfactory to assign integral values to the monomer and dimer elution rates. The integral rates were chosen such that their ratio corresponded to the ratio exhibited by elution positions of the monomer and dimer experimentally; the number of cells used to represent the column was adjusted accordingly. However, because the current simulation models univalent and bivalent interactions of molecules that may each elute with different velocity, four different velocities for the collection of eluting species are required. Therefore, the earlier strategy was abandoned. These velocity parameters correspond to the constituent velocites in the early transport analyses of Gilbert & Jenkins (1959) and Nichol and Ogston (1965).

Previously, the content of a protein species in cell i was transferred to cell $i + v$, where v was the integral velocity of the species. Currently, the term *cell i* refers to the cell located between positions $i - 0.5$ and $i + 0.5$; the content of cell i is translated to cells j such that the center of mass position is at $i + v$ (Figure 1). It is assumed that a Gaussian (normal) distribution function represents the distribution of the protein about position $i + v$. Adoption of this strategy adds two significant attributes to the algorithm. First, fractional values of velocity can be assigned, facilitating systems incorporating multiple-elution velocities. Second, the Gaussian distribution introduces a standard deviation factor, which is taken to approximate the dispersion parameter described above.

In practice, the translations are accomplished by reference to a table of normal distribution values. Values from 0.00 to 3.49 standard deviations are included in the computer program as a data statement, and the corresponding values from 0.0 to −3.49 standard deviations are generated. By means of interpolation between these entries, the protocol, in principle, is able to distinguish velocity differences of 0.001 cell/cycle (c/c). Translation of cell i content to any cell j is effected then by indexing the $j - 0.5$ and $j + 0.5$ positions on the basis of the center of mass position $i + v$ and the standard deviation. The content of cell j, $c(j)$, becomes

$$c(j) = c(i)[F(j + 0.5) - F(j - 0.5)]$$

where $F(x)$ represents the interpolated distribution function value at position x, obtained by reference to the table. This procedure is applied to cells within at least three standard deviations about the mean position. The translation routine is applied to each of the two interactive components separately. The expression of complex formation is described below.

Univalent Interaction. The interaction between two proteins is incorporated into the algorithm by effecting an equilibration step between cycles of translation. The concentration of complex formed by proteins A and B is determined on the basis of the standard relationship

$$c = K_a ab$$

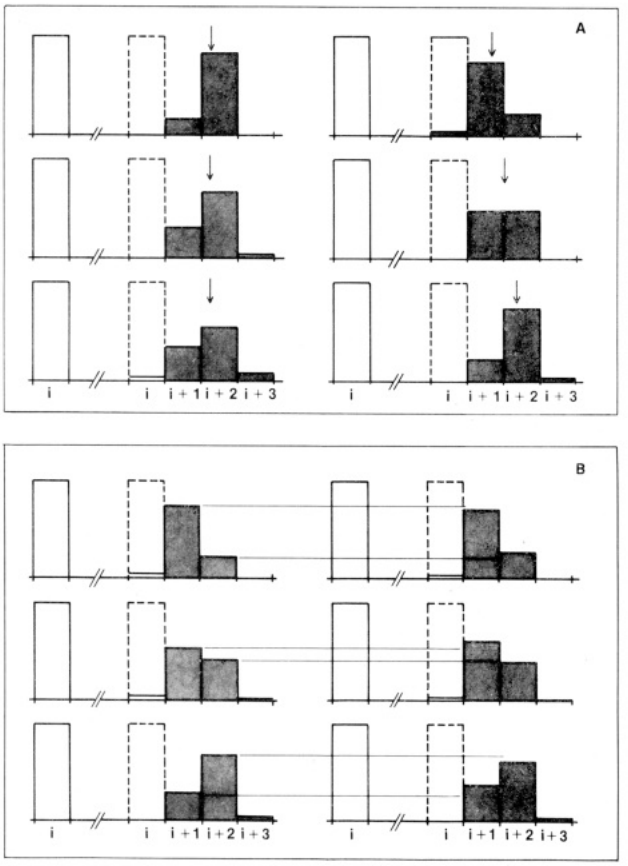

FIGURE 1: Demonstration of the translation routine. (A) Translation of the contents of cell i as a function of the dispersion factor (σ), left panel, and the velocity (V), right panel, respectively. In the left panel, from top to bottom, $\sigma = 0.2$, 0.4, and 0.6 cell for $V = 1.7$ c/c; in the right panel, $V = 1.2$, 1.5, and 1.8 c/c for $\sigma = 0.4$ cell. The arrow indicates the center of mass position. (B) Role of the association constant K_a in determining the outcome of the translation of monovalently interacting proteins in cell i present at initial concentrations of 0.1 μM; $V(1) = V(2) = 1.2$ c/c, $V(3) = 1.7$ c/c, and $\sigma = 0.4$ cell. From top to bottom, $K_a = 10^5$, 10^7, and 10^9 M^{-1}. The left panel represents the distribution resulting from separate translation of free and complexed species; the right panel assumes a time-averaged interconversion of free and complexed species during the translation cycle.

where a and b represent the equilibrium molar concentrations of the two interacting species and c represents that of the complex; K_a is the association constant. For numerical convenience, the equation is made unitless

$$c' = a'b'$$

by multiplying each side of the expression by K_a. This leads to

$$c' = \{(1 + a_0' + b_0') - [(1 + a_0' + b_0')^2 - 4a_0'b_0']^{1/2}\}/2$$

where a_0' and b_0' represent the total unitless molar concentrations of the interacting species. Finally

$$c = c'/K_a$$

The value of c directly yields a and b:

$$a = a_0 - c$$

$$b = b_0 - c$$

The usual assumption is made that equilibration between cycles is effectively instantaneous. A corollary to this assumption is the expectation that all molecules of each species participate in a complex during each cycle. Consequently, population A, rather than existing as a free subpopulation with velocity v_a and a complexed subpopulation with velocity v_c, is considered to exist as a homogeneous population with constituent velocity

$$\bar{v}_a = (av_a + cv_c)/(a + c)$$

or

$$\bar{v}_a = (av_a + cv_c)/a_0$$

and

$$\bar{v}_b = (bv_b + cv_c)/b_0$$

Likewise, mean dispersions are calculated:

$$\bar{\sigma}_a = (a\sigma_a + c\sigma_c)/a_0$$

and

$$\bar{\sigma}_b = (b\sigma_b + c\sigma_c)/b_0$$

These averaged values of velocity and dispersion are used to individually translate species A and B along the column. An average diffusion parameter is similarly obtained and used in the diffusion routine of the algorithm. It should be recognized that the expressions for mean dispersion and diffusion are approximations. Since the dispersion and diffusion parameters for the complex are estimated from the corresponding values of the constituents and their relative velocities, use of this approximation is considered justified at this time. However, improvement in the evaluation of the characteristics of the complex will enable a more rigorous definition of the dispersion and diffusion properties of the mixture. This problem has been discussed in some detail by Cox and Dale (1981).

Bivalent Interaction. In the case of bivalent interaction, it is assumed that the two binding sites are independent and equivalent, as may be expected in studies of monoclonal antibody and homogeneous antigen. No attempt is made to approach characterization of cooperative or heterogeneous binding. The immediate consequence of bivalency in one of the interacting components is that the effective molar concentration of that component is doubled. The resulting concentration c is then more conveniently interpreted as the concentration of complexed binding sites rather than the concentration of complexes. In the case of a bivalent interaction, two types of complex are present. If A is the bivalent species, complexes of types AB and BAB are both formed. Together with free A and free B, four species characterize the interacting mixture. The distribution of free and complexed molecules is calculated by considering the fractional occupancy of binding sites

$$f = c/(2a_0)$$

as the probability that a given binding site is occupied. Accordingly, the concentration of AB complex (c_1) is given by

$$c_1 = 2f(1 - f)a_0$$

that of the BAB complex (c_2) by

$$c_2 = f^2a_0$$

while the free A concentration is

$$a = (1 - f)^2a_0$$

The expression for the concentration b remains as above.

Given the distribution of free components and the two types of complex, the average velocities and dispersion parameters are calculated. The expressions for velocity become

$$v_a = (av_a + c_1v_{c1} + c_2v_{c2})/a_0$$

and

$$v_b = (bv_b + c_1v_{c1} + 2c_1v_{c2})/b_0$$

Expressions of the same form are obtained for the dispersion and diffusion parameters. These expressions are then used in the translation routine to calculate the displacement of components A and B.

Monitor. The terminus of the simulated column is supplemented with a short series of cells designated the monitor queue. The purpose of this segment is 2-fold: (1) to provide correspondence with the "dead volume" between the terminus of the column and the detector and (2) to translate each species at unitary velocity through the monitor. The protein contents of the terminal cell of the queue are multiplied by the appropriate extinction coefficient, and the sum of the absorbances is recorded. As a result, the series of values determined at the monitor queue terminus corresponds to the time-dependent reading at an optical monitor during the development of an experimental chromatogram.

Application of the Simulation. The first step in relating simulated data to an experimental chromatogram is to determine the parameters necessary to emulate the profiles exhibited by the interacting species when chromatographed individually. This consists of obtaining values for the velocity, dispersion, and diffusion parameters that optimize correspondence between the observed and calculated elution profiles. The correlation coefficient between simulated and experimental profiles is used as the objective statistic for evaluating this correspondence. The correlation coefficient is sensitive to the shape and positions of the respective elution peaks. Additional criteria for future evaluation may include variance and segmental weighting with specific attention to avoidance of bias introduced by experimental skewness of the elution profile.

For each component of the system, initial values for dispersion and diffusion parameters are selected, and the velocity parameter is varied in sequential runs to maximize the correlation with the experimental chromatogram. This value is then fixed, while the dispersion and diffusion parameters are varied to further improve the correlation. At this point, iterative simulations of a mixture of the two components are obtained with the above-determined parameters held fixed. The value of K_a is varied to obtain the optimal correlation. This value of K_a is subsequently tested by examining its predictive value for experimental runs at different concentrations of the interacting species.

An additional aspect of the interaction is contained in what may be termed the delta. Experimentally, this is the difference (delta) between the arithmetic summation of the profiles of the two components chromatographed separately and the chromatogram obtained with a mixture of the two species. In the simulation, the delta is taken as the difference between the chromatogram of two nonassociating components (K_a = 0 M^{-1}) and that obtained for any other K_a. The delta is, thus, a polymodal distribution function, with a positive leading component attributed to the forward time displacement of the complex or complexes and a trailing negative component(s) reflecting the removal of the species forming the complex.

Results

Characterization of the Simulation. Simulation of protein migration through the column is accomplished by successive translation steps in the algorithm. As illustrated in Figure 1, the contents of cell i are moved to cell $i + x$ and flanking cells as controlled by the dispersion coefficient. The mean (center of mass) position is $i + v$, with v the velocity parameter of the species translated. The content of any given cell j is the product of the content of cell i and the integrated Gaussian distribution between position $j - 0.5$ and $j + 0.5$. Figure 1A displays the dependence of this translation upon the dispersion parameter (left panel). The center of mass position is constant while the content of the modal cell decreases and that of the flanking cells increases. The dependence upon v is illustrated in the right panel of Figure 1B, demonstrating the forward shift of the center of mass position for increasing v with a fixed σ value.

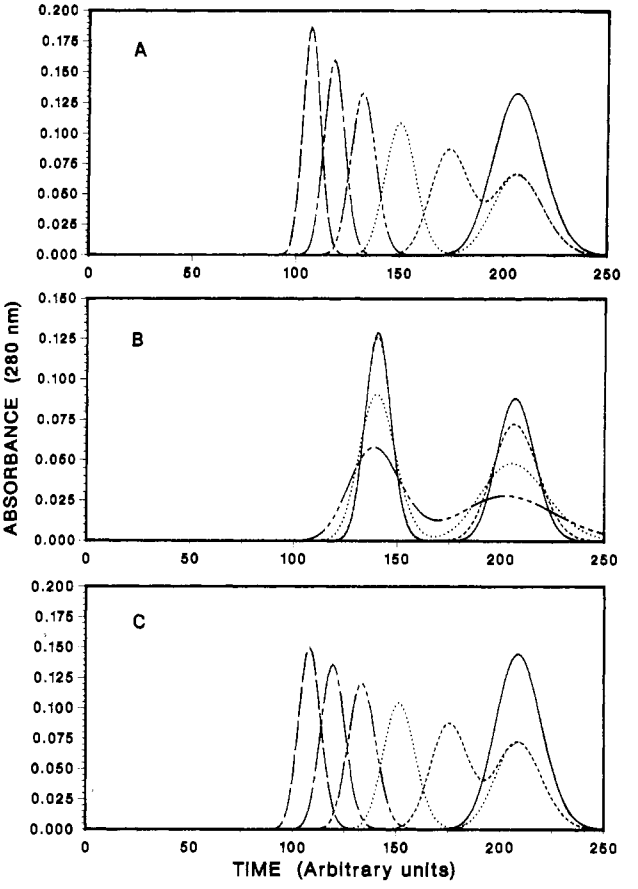

FIGURE 2: Simulated column runs illustrating the effect of velocity (A) and dispersion (B) parameters on calculated elution profiles. In Figures 2–4, CL = 200 cells and RL = 250 cycles. In (A), the dispersion parameter is fixed and equal for the two simulated species, resulting in narrower elution profiles for values of increasing linear velocity. Profiles generated with dispersion values increasing with linear velocity are shown in (C). (A) $V(1)$ = 1.0 c/c, $\sigma(1) = \sigma(2)$ = 0.40 c, and $V(2)$ = 1.0 c/c (—) on $V(2)$ = 2.0 c/c (– –); intermediate values in steps of 0.2 c/c. (B) $V(1)$ = 1.0 c/c, $V(2)$ = 1.5 c/c, $\sigma(1)$ = 0.2 c (—), and $\sigma(2)$ = 0.4 c (- - -), $\sigma(2)$ = 1.0 c (···), on $\sigma(2)$ = 1.5 c (– –). (C) $V(1)$ = 1.0 c/c, $\sigma(1)$ = 0.4 c, $V(2)$ as in (a), and $\sigma(2) = \sigma(1)$ $[V(2)/V(1)]$.

Figure 1B illustrates the relationship of K_a to the resulting translational distribution of the content of cell i. The concentrations of components A and B are arbitrarily taken as 0.1 μM with velocity v = 1.2 c/c; the K_a is varied from 0 to 10^7 M^{-1}. The weighted average velocity is indicated for each case. The two panels in Figure 1B illustrate the two translation strategies referred to earlier. The left side depicts the distribution pattern obtained if free and complexed forms are translocated discretely; the right panel represents the consequence of continuous "instantaneous" reequilibration in which all molecules of the population participate in complex formation. It should be noted that in each case the center of mass displacement is the same, but the two approaches generate somewhat different final distributions of protein.

Simulated Chromatograms. Figures 2–4 show elution profiles from a series of simulated column runs. To illustrate

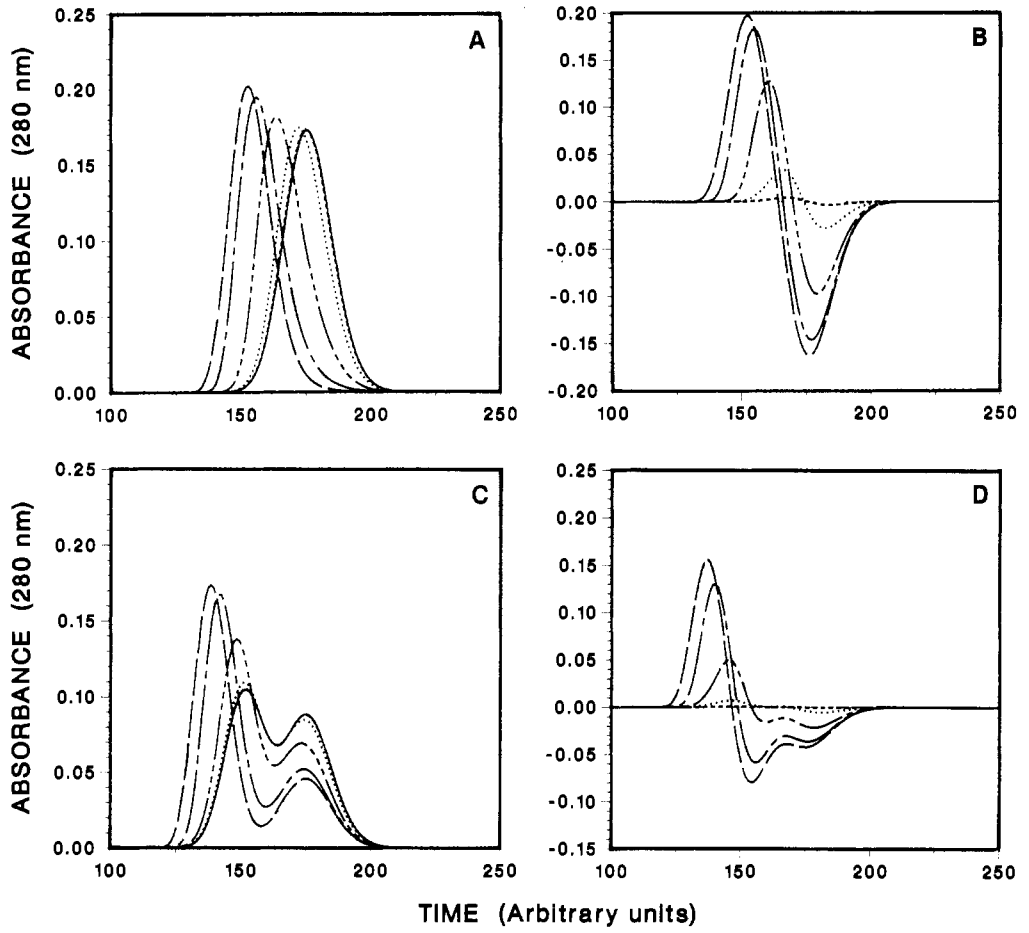

FIGURE 3: Simulated association profiles illustrating (A) molecular self-association or complex formation by molecules of equal molecular weight and elution velocity and (B) the deltas constructed by the differences of these profiles relative to the $K_a = 0$ M^{-1} profile. The association process results in a characteristically sharp leading edge in the elution profile. Valence = 1. $V(1) = V(2) = 1.2$ c/c, $V(3) = 1.4$ c/c, $\sigma(1) = \sigma(2) = 0.50$ c, and $\sigma(3) = 0.58$ c. Simulated association profiles illustrating complex formation by two species of different molecular weights resulting in a forward shift of the elution profile (C) and a polymodal delta (D). Valence = 1. $V(1) = 1.2$ c/c, $V(2) = 1.4$ c/c, $V(3) = 1.56$ c/c, $\sigma(1) = 0.50$ c, $\sigma(2) = 0.58$ c, and $\sigma(3) = 0.65$ c. $K_a = 0$ M^{-1} (—), $K_a = 10^4$ M^{-1} (···), $K_a = 10^5$ M^{-1} (- - - -), $K_a = 10^6$ M^{-1} (— - —), and $K_a = 10^7$ M^{-1} (– –).

the effects of different variables, profiles were generated for several values of the velocity and dispersion parameters for noninteracting proteins. The dependence of the elution profiles and resulting deltas for associating species is depicted for a range of K_a. Examples of monovalent and bivalent interactions for proteins of equal and divergent elution velocites are presented.

(*A*) *Noninteracting Components.* Figure 2A characterizes simulated mixtures of two noninteracting proteins. The velocity of a reference protein is kept fixed while the velocity of the second species is sequentially incremented to a final value twice that of the reference species. The sharpening of the profile of the more rapidly migrating component with increasing velocity results from allowing σ of this species to remain fixed. In Figure 2B, the effect of the dispersion coefficient on the generated elution profiles for two species of distinct fixed velocites is illustrated. Figure 2C is essentially a reprise of the conditions of Figure 2A, except that the dispersion factor of species 2 is allowed to vary with the linear velocity of species 2; i.e., $\sigma_2 v_1 = \sigma_1 v_2$. Although broadening of the first peak relative to its counterpart in Figure 2A is apparent, sharpening of the peak is still observed. This finding suggests a second component contributes to the total dispersion obtained by the algorithm. This second component is, in fact, numerical dispersion and will be discussed in more detail later.

(*B*) *Interacting Components of Equal Molecular Weight.* Figure 3 shows the effect of K_a on the elution profiles exhibited by two interacting species. As is characteristic of an aggregating system, and most pronounced in the case of self-association or aggregation of molecules of equal molecular weight, the elution profiles exhibit asymmetry under conditions of observable interaction (Figure 3A). This asymmetry, first described by Winzor and Scheraga (1963), takes the form of a sharply ascending leading edge and a trailing edge extending to the trailing edge position obtained in the case of nonassociation. The position of the trailing edge follows from the fact that in any system at equilibrium, a fraction of the interactive species is in a free, unassociated state. The asymmetry of the profile results from concentration-dependent association leading to a higher average molecular weight within the solute band than that at either the leading or the trailing edge. Therefore, the average velocity within the band varies with concentration, causing the solute peak to elute closer to the leading edge than to the trailing edge. This phenomenon is association/dissociation driven and is, accordingly, less visible at low and high extremes of K_a. Further, the appearance of this asymmetric profile may be taken as evidence that the reverse rate constant is rapid relative to the elution velocity of the solute.

(*C*) *Delta Profiles.* Figure 3B displays the deltas characterizing the interaction profiles of Figure 3A. Qualitatively, the magnitude of the delta increases with increasing K_a. The shape of the delta is characterized by positive and negative components reflecting a forward shift due to complex for-

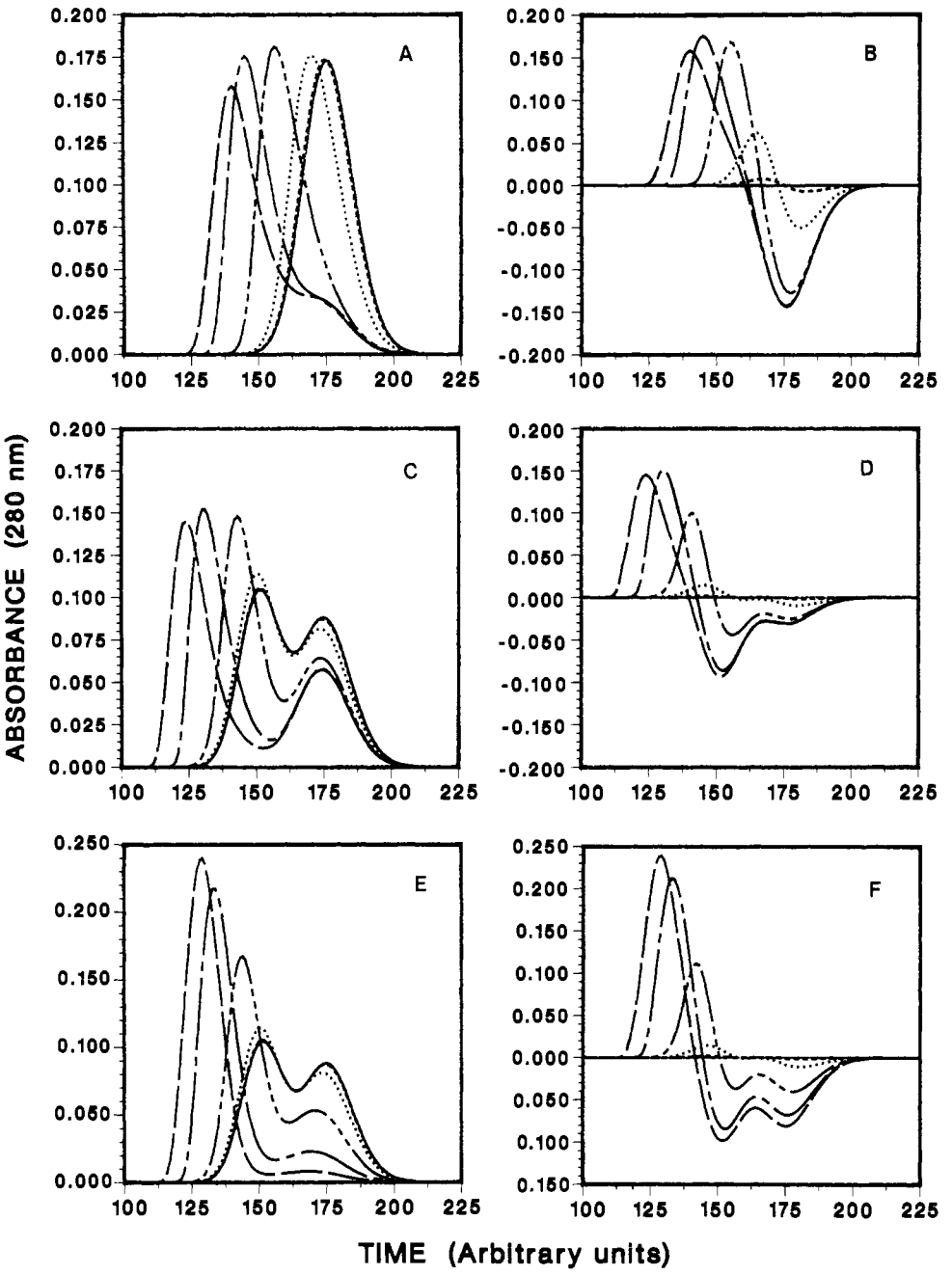

FIGURE 4: Simulated association profiles. Bivalent interactions are demonstrated for molecules of equal molecular weight (A and B) and resolvable molecular weights in which the bivalent molecule is the larger component (C and D) or the smaller (E and F). Valence = 2. (A and B) $V(1) = V(2) = 1.2$ c/c, $V(3) = 1.4$ c/c, $V(4) = 1.56$ c/c, $\sigma(1) = \sigma(2) = 0.5$ c, $\sigma(3) = 0.58$ c, and $\sigma(4) = 0.65$ c. (C and D) $V(1) = 1.2$ c/c, $V(2) = 1.4$ c/c, $V(3) = 1.56$ c/c, $V(4) = 1.81$ c/c, $\sigma(1) = 0.50$ c, $\sigma(2) = 0.58$ c, $\sigma(3) = 0.65$ c, and $\sigma(4) = 0.75$ c. (E and F) $V(1) = 1.4$ c/c, $V(2) = 1.2$ c/c, $V(3) = 1.56$ c/c, $V(4) = 1.69$ c/c, $\sigma(1) = 0.58$ c, $\sigma(2) = 0.50$ c, $\sigma(3) = 0.65$ c, and $\sigma(4) = 0.70$ c.

mation complemented by the depletion of associating molecules from the lower molecular weight zone. The positive and negative components are equal in magnitude. The unimodal structure of the positive and negative components in Figure 3B is a consequence of a homogeneous complex and a single velocity characterizing both of the interacting species.

(D) Interacting Components of Different Molecular Weights. An alternative set of circumstances is explored in Figure 3C in which the interacting species have different elution velocities. Thus, the resulting elution profiles are the outcome of two countervailing trends during the development of the chromatogram. In this case, the association process is attenuated by the ability of the column to separate the two interactive species. The elution profiles thus generated are shown in Figure 3C for the same series of K_a values used to generate Figure 3A.

The delta profiles obtained for solutes of different molecular weight (Figure 3D) show two general differences in comparison with the deltas obtained in Figure 3B. First, for each K_a, the magnitude of the delta is less than the delta obtained for interacting species of the same elution velocity. Second, the negative component of the delta has a bimodal character, which is the outcome of depleting two zones of lower molecular weight solute. The positive component remains unimodal, as only one type of complex is formed in this example. It should be noted that the delta is itself the sum of two deltas, one for each of the two interacting components.

(E) Bivalent Interaction. The illustrations in Figure 3 depicted the two classes of univalent interactions. There are three types of bivalent interaction if bivalency is restricted to only one of the components. This set of three conditions includes interacting molecules of equal elution velocity and

interactions between molecules of different elution rates in which either the monovalent or bivalent component may be the more rapidly eluting partner. Representative simulated profiles of each of these conditions are shown in Figure 4.

Figure 4A,B depicts the elution profile and delta obtained for equal-sized proteins. A low molecular weight shoulder is evident for high values of K_a. This is a consequence of bivalency by which one of the components is in a 2-fold molar excess. As a result, some of the bivalent molecules do not form a complex and, thus, migrate as a free species. In the succeeding figures, elution profiles and deltas for proteins of unequal molecular weight are presented. In these cases, the bivalent partner is of lesser (Figure 4C,D) or greater (Figure 4E,F) molecular weight. The earlier elution positions noted in Figure 4C compared to Figure 4E result from the formation of larger molecular weight complexes with the smaller component binding two large components. However, the feature that most significantly distinguishes the two sets of data is the ability of the interaction in the latter circumstance, bivalent high molecular weight component, to deplete the late-eluting peak. This difference results from the molar ratios of binding sites in the two cases. In the case of a bivalent low molecular weight component, the species already in molar excess on the basis of equal mass concentration is effectively doubled in concentration. Consequently, even at high values of K_a, a significant fraction of this species is not in a complex at the start of a column run. In the opposite case, bivalency of the larger molecular weight component results in a molar balance of the two reactants.

Experimental Interaction Profiles. (A) Anti-Idiotypic Antibody. To test the qualitative and quantitative validity of the simulation features described above, the model was applied to several cases of experimental antibody–antigen interactions. Figure 5 depicts an experimental demonstration of perturbation of an elution profile due to the formation of a complex between two different antibody fragments. One of these, the antigen, is the F(ab′) derived from the murine myeloma IgA T-15. The other component of the interactive system is the F(ab′) derived from the murine hybridoma monoclonal antibody F-6 and is directed against an idiotypic determinant of T-15 (Wittner et al., 1982).

Figure 5A summarizes chromatograms obtained for the two proteins when they were applied individually to a column of Superose-12. The T-15 F(ab′) appears to have a somewhat larger molecular weight than that of the F(ab′) obtained from the IgG F-6. Each profile also reveals a small amount of higher molecular weight material, possibly residual $F(ab')_2$. Figure 5B compares the elution profile of an experimental mixture of F-6 and T-15 with the synthetic profile obtained by summation of the two profiles displayed in Figure 5A. A substantial difference is exhibited by the mixture when compared to the synthetic "zero-interaction" profile. The delta profile exhibits the positive and negative components discussed above. Further, the negative lobe of the delta appears unimodal, reflecting the similarity of the elution velocities of the interacting components. The magnitude of the negative lobe is a significant fraction of that of the peak representing the mixture. The T-15 and F-6 chromatograms thus demonstrate the basic principle of small-zone interactive chromatography, which is that the interaction between two proteins can result in a measurable perturbation in the elution behavior of a mixture of the interacting components.

(B) Rheumatoid Factor. Experimental results analogous to the simulated elution profiles of Figure 3 are shown in Figure 6. In contrast to the preceding example (Figure 5)

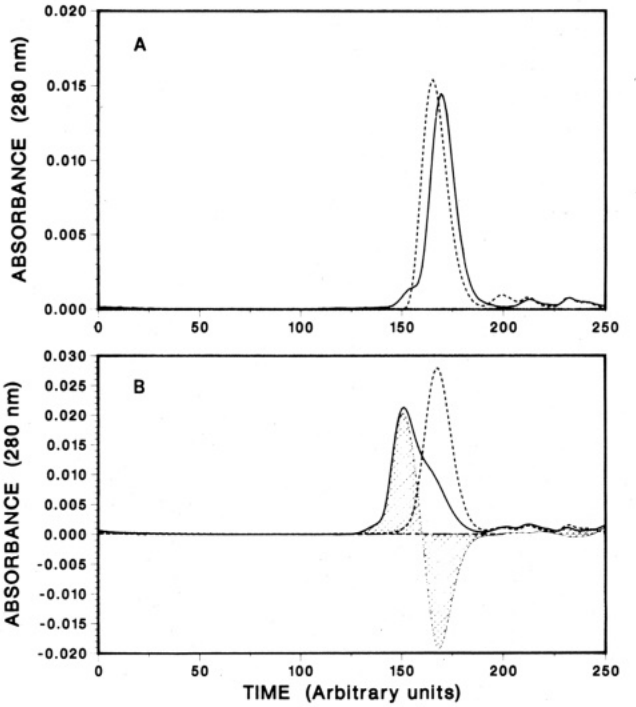

FIGURE 5: Chromatogram of interaction. (A) Elution profile of Fab′ preparations of T-15 and F-6 chromatographed on Superose 12. Initial concentrations 0.1 mg/mL. Run time is 60 min at a flow rate of 0.06 mL/min. F-6 Fab′ (—), T-15 Fab′ (- - -) (B) Summation (- - -) of the elution profiles shown in (A) compared to the experimental chromatogram obtained with a mixture of T-15 and F-6 (—). The delta (hatched) is constructed by subtraction of the summed elution profile from the profile of the mixture.

in which the interacting Fabs were of approximately equal size and effectively co-eluted whether associated or dissociated, the elution profiles summarized in Figure 6A–C were obtained with interacting molecules of unequal size and elution velocities. The molecules used were the Fab derived from the human IgA RF (SCH) and the intact monoclonal human IgG_1 (DRI). The molecular weight ratio of the IgG to Fab is approximately 3:1, resulting in a significantly faster elution velocity for the intact molecule. The interaction between the RF Fab and IgG is depicted in Figure 6B. As illustrated in the simulation (Figure 3), the interaction between solutes of divergent elution velocities results in a polymodal delta, although in this particular experimental example the positive component is the bivalent lobe. Deltas obtained at three other sets of solute concentrations are shown in Figure 6C. The interaction between the RF and its antigen is examined in more detail below.

The chromatogram and deltas represented in Figures 5 and 6 may be used to illustrate qualitative interpretation of the small-zone profiles. The antibodies and fragments were essentially homogeneous. However, the relative magnitude of the delta for the T-15–F-6 interaction (Figure 5) exceeds the delta of the RF-IgG–RF-Fc interaction (Figure 6) even though the concentrations in the T-15–F-6 example are approximately 10-fold lower. The observation that the complexes formed in the RF-Fc runs do not elute at the position appropriate for an aggregate 2 or 3 times the size of the Fc or Fab (as indicated by the positive lobe of the delta) further suggests a relatively low K_a for this interaction. Concentration-dependent dissociation and reassociation occur throughout the course of the run, resulting in an intermediate elution position between that expected for a complex and that for nonassociating monomers. However, reassociation is limited in the case of solutes of nonequal molecular weight (Figure 7) by the ability of the

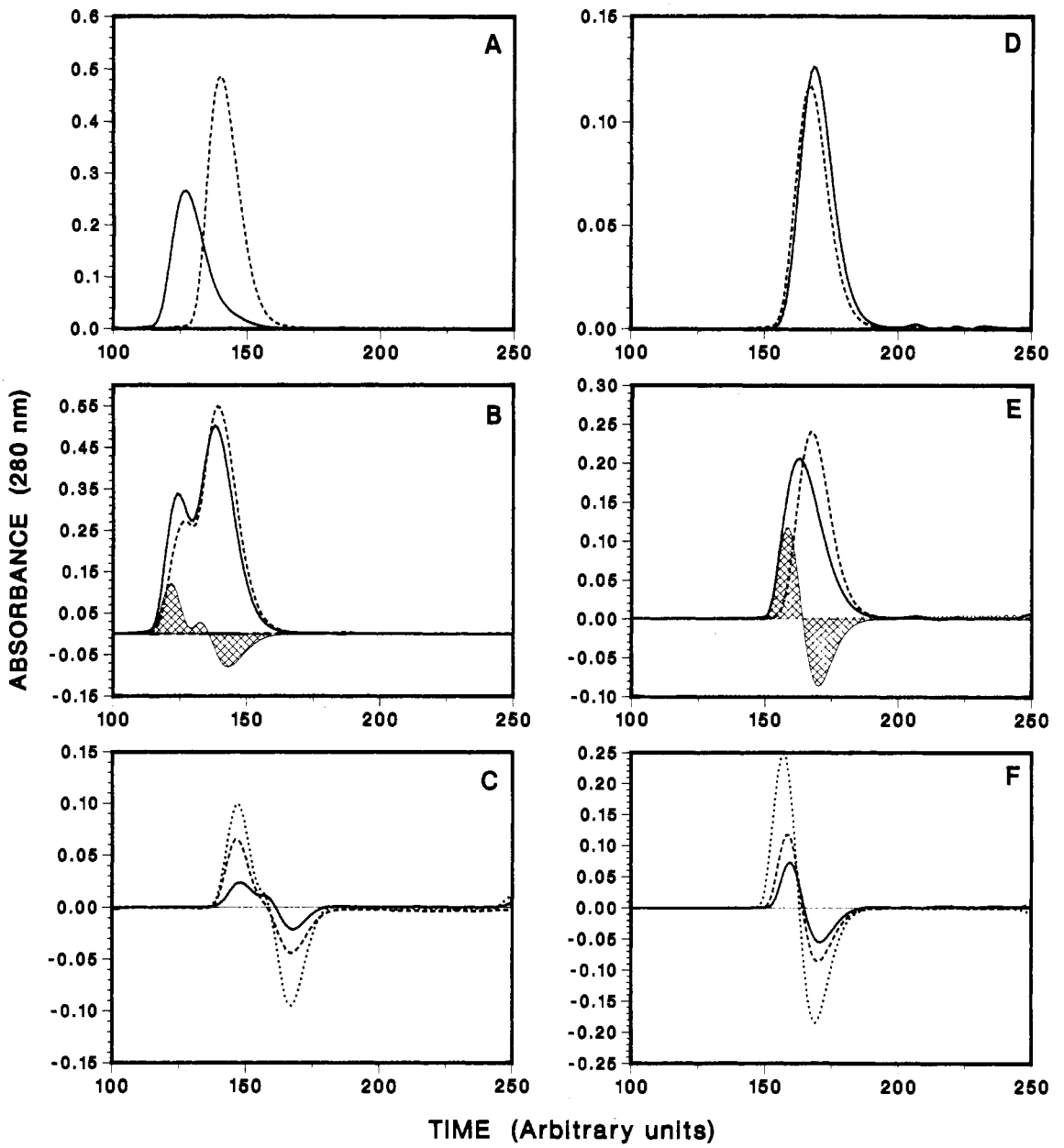

FIGURE 6: Chromatogram of interaction. (A) Elution profiles of SCH Fab [4.70 mg/mL (---)] and DRI IgG [2.82 mg/mL (—)] chromatographed individually on Superose 12; flow rate 0.06 mL/min; run time 40 min. (B) Comparison of the chromatogram obtained with a mixture of Fab and IgG (—) and the synthetic profile obtained by summation (---) of the two profiles in (A). (C) Deltas obtained from the RF IgG mixture at three sets of concentrations: Fab:IgG 0.94:2.82 mg/mL (—), 0.94:1.41 mg/mL (---), and 2.35:2.82 mg/mL (···); flow rate 0.033 mL/min run time 60 min. The bimodal nature of the positive component of the delta profile is more prominent for some concentration sets than others. (D) Elution profiles exhibited by SCH Fab (---) and DRI Fc (—) chromatographed individually on Superose 12: flow rate 0.033 mL/min; run time 60 min. (E) Comparison of the chromatogram obtained with a mixture (—) of Fab and Fc and the synthetic profile obtained by summation (---) of the two profiles in (A). (F) Deltas obtained from the RF Fc mixture at three sets of concentrations (Table I), illustrating increased magnitude at higher concentrations: I (—) < II (---) < III (···).

column to separate the interacting molecules when dissociated. Thus, in addition to K_a and the initial solute concentration, the delta can be expected to be a function of the length of the column, the flow rate, the relative sizes of the solutes, and the partitioning properties of the chromatographic matrix.

(C) Application of Simulation. The simulation procedures were quantitatively applied to analyze an interacting protein system consisting of the Fab derived from SCH and an Fc prepared from DRI. The comparable sizes of these molecules resulted in similar elution velocities and maximized the magnitude of the observed interaction. Results of chromatographic analyses of mixtures of the RF Fab and Fc are shown in Figure 6D–F. Chromatograms were obtained at three different concentrations/ratios of the interacting components. One set is shown in Figure 6D, illustrating individual runs of the two components. The delta for this experiment is constructed in Figure 6E. A summary of the deltas observed in each of the three concentration sets is found in Figure 6F.

The elution behavior of the Fab Fc mixture was modeled for each of the initial concentration values. A comparison of simulated and experimental elution profiles for optimized parameters is shown in Figure 7. In this analysis, the nominal protein concentrations determined by absorbance at 280 nm were used as the initial sample concentrations in the simulation. No effort was made to adjust the simulated value of concentrations or extinction coefficients to the experimental values in order to improve the correspondence between the two data sets. A 280-nm absorbance value of 1.0 per 1 mg/mL concentration was assumed for both the Fc and Fab components. If the extinction coefficients of the two interacting components

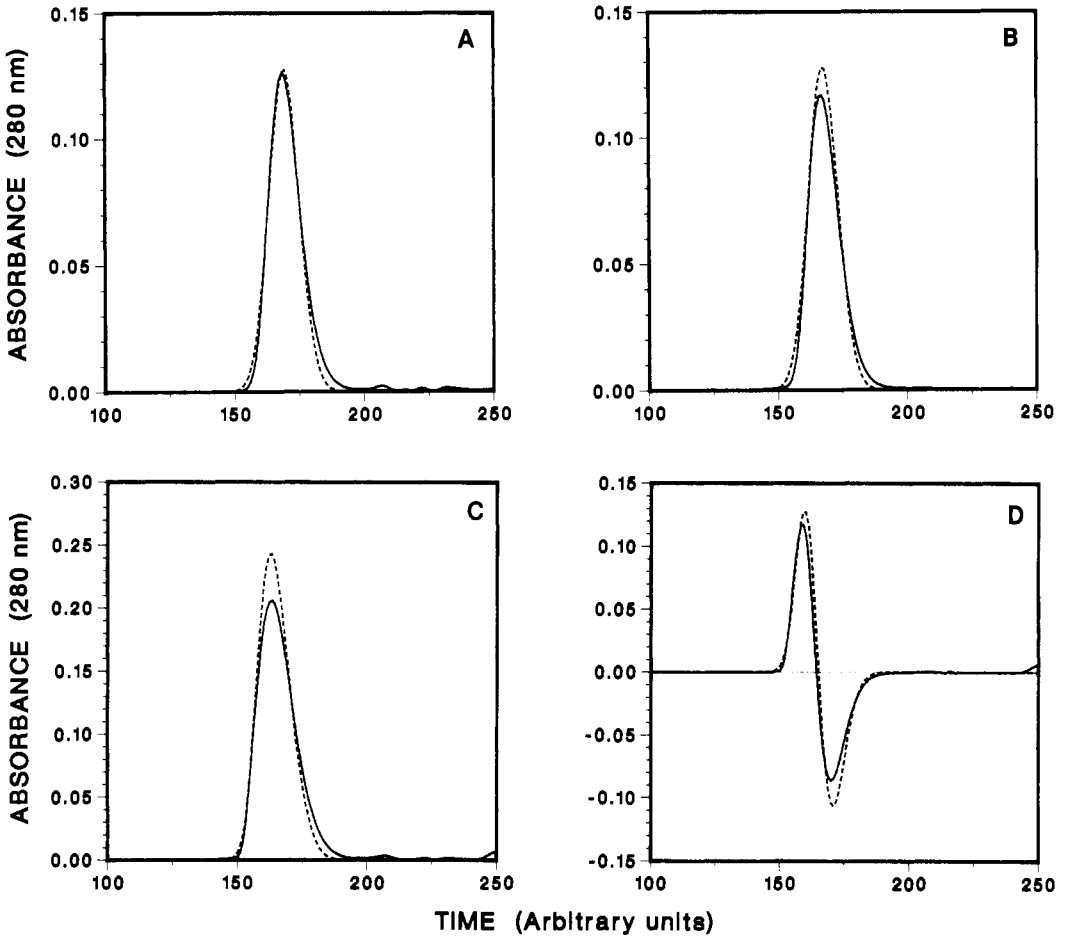

FIGURE 7: Comparison of simulated and experimental elution profiles. (A) A correlation coefficient of 0.9970 was obtained between the experimentally observed elution pattern exhibited by DRI Fc (—) and the simulated profile (---) resulting with a velocity parameter of 1.412 c/c. (B) A correlation coefficient of 0.9972 was found for velocity parameter of 1.424 c/c in simulating (---) the experimental elution profile of SCH Fab (—). (C) The elution profile exhibited by a mixture of SCH Fab and DRI Fc (—) is compared with a simulated profile (---) generated with a K_a value of 1.4×10^5 M^{-1}. The correlation between experimental and calculated profiles is 0.9955. (D) Comparison of deltas constructed for experimental (—) and simulated elution (---) profiles. The correlation coefficient between the two deltas is 0.9810. The simulated column had a length of 225 cells and a monitor queue of 9 cells. Each simulated protein had a dispersion factor of 0.40 and a diffusion parameter of 0.07.

are in fact equal, then variance of the assumed value from the actual value results in a shift in the absolute value of the estimated K_a inversely related to the shift in the resulting estimated concentrations of the interacting components. This error does not qualitatively affect the correspondence of the simulation to the experiment. On the other hand, if the ratio of the concentrations of the two experimental components is different from that used in the simulation, then a concentration-dependent systematic error may be expected. The absolute concentrations of the SCH Fab and DRI Fc will receive more attention in a subsequent paper focused on the properties of these molecules rather than on the characteristics of the simulation.

(*D*) *Estimation of Rheumatoid Factor* K_a. Figure 7C compares the experimental and simulated results for the mixture of Fab and Fc. The elution velocity of a complex of one Fc and two Fabs was taken as that of an IgG on the same column; the velocity of a complex of one Fc and one Fab was estimated from the elution position predicted by the standard curve constructed from the elution positions of Fab, Fc, and IgG (data not shown). A correlation coefficient of 0.9955 was obtained with a K_a value of 1.35×10^{-5} M^{-1} with the valence of Fc DRI assumed to be 2. A valence assumption of 1 yielded a maximum value for the correlation coefficient of 0.9943 at a K_a value of 4.0×10^5 M^{-1}. The difference in the correlation coefficients obtained for the two estimated values of K_a cannot be considered significant and, hence, does not itself provide a basis for choice of correct K_a and valence. In general, it is expected that a single experimental set of component concentrations will provide two equally suitable choices for the values of the valence and association constant unless the elution profile has been significantly determined by the presence of a rapidly eluting trimeric component.

Table I: Optimized K_a Values: SCH–DRI Interaction

	concn[a]		K_a[b] (correl coeff)	
set	Fab	Fc	valence = 1	valence = 2
I	0.94	0.46	2.4 (0.9958)	1.10 (0.9969)
II	0.94	0.92	4.0 (0.9943)	1.35 (0.9955)
III	2.35	0.92	7.0 (0.9910)	1.70 (0.9943)
			4.5 (0.9937)[c]	1.38 (0.9956)[c]

[a] mg/mL. [b] $\times 10^{-5}$ M. [c] Average.

To resolve the ambiguity, the mixture of RF Fab and IgG Fc was run at two other concentrations and ratios (Table I). The delta profiles resulting from the three runs are presented in Figure 6F. Simulations were executed for the second and third sets of concentrations assuming an Fc valence of 1 and an Fc valence of 2. It was anticipated that correct estimates of K_a and valence would result in better correlations between simulated and experimental data at all three concentration conditions. Expressed differently, values of K_a obtained to maximize correlation coefficients at multiple concentrations

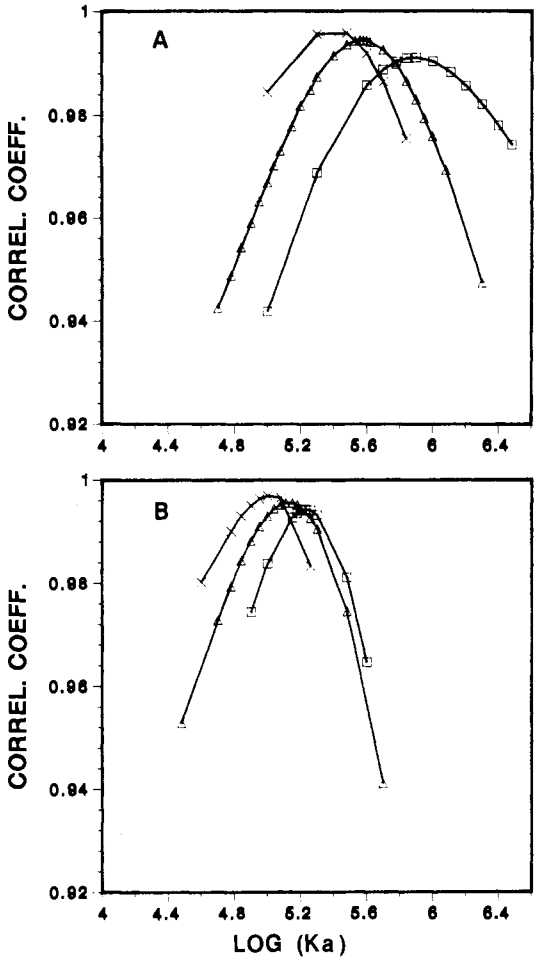

FIGURE 8: Interaction valence. The correlation coefficients obtained between simulated and experimental elution profiles of mixtures of SCH Fab and DRI Fc at three sets of concentrations assuming an antigen valence of 1 (A) and 2 (B) for the Fc. Data sets: I (×), II (△), and III (□). The correlation coefficient values are plotted as a function of log K_a.

will demonstrate less variance in the case of an appropriate value for the interaction valence.

Figure 8 depicts the results of these simulations. The correlation coefficient as a function of log K_a is plotted for the three experiments with an assumed antigenic valence of 1 (Figure 8A) and 2 (Figure 8B) for the Fc. These results clearly indicate that less variance in the estimated optimal values of K_a was obtained with the valence of the Fc taken to be 2. As summarized in Table I, the estimated values of K_a ranged from 1.1×10^5 to 1.7×10^5 M^{-1} under this assumption; whereas the range of the K_a estimates for a valence of 1 was found to be $(2.4\text{–}7.0) \times 10^5$ M^{-1}. In addition, the maximum correlation values found for the univalent assumption were consistently less than those obtained with the bivalent assumption.

Discussion

Validity of the Simulation. The primary purpose for developing this simulation of small-zone chromatography of interacting proteins was to provide a tool that could be routinely used for a series of studies on the binding of antibodies and their fragments to macromolecular protein antigens. In the present investigation, the values for K_a obtained for the interaction between the RF Fab SCH and the IgG Fc DRI assuming an antigenic valence of 2 were self-consistent, those obtained with an assumed valence of 1 were not. In the latter case, a 5-fold range in the product of solute concentrations required a 3-fold range of K_a in the simulation to optimize the fits with the experimental data. A combination of invalid assigned valence or K_a is unlikely to generate chromatography simulations that fit experimental elution profiles over a range of starting solute concentrations. As a result, the observed consistency of the K_a obtained with a valence value of 2 supports the validity of the simulation procedure.

Validity of the simulation procedure is dependent upon the soundness of the assumptions used in the model and the soundness of the computational algorithm used to depict this model numerically. The central assumption is that the chromatography column need not be described mechanistically but instead is amenable to a phenomenological representation. To the extent that it is possible to mirror the elution rates and band-spreading characteristics of interacting solutes A and B, the concentration of complex C can be calculated from first principles and also translocated appropriately. The ability of the algorithm to generate simulated elution profiles of the independently chromatographed Fab and Fc that correspond to the experimental profiles with correlation coefficients in excess of 0.995 suggests that, at least to a first approximation, this assumption is fulfilled. The secondary assumption that equilibration is rapid relative to the rate of transport is not essential for the application of this simulation strategy. This assumption will be eliminated for analyses of high-affinity interactions, in which the large K_a value may be achieved by a small dissociation rate constant.

Effect of Dispersion. However, there remains the possible influence of numerical dispersion on the expression of the algorithm. Cox (1978) has pointed out that numerical dispersion is a general problem "affecting finite difference simulations of all kinds.". The simulation described in this paper is no exception. This intrinsic dispersion may be observed in Figure 1B, in which for velocity parameters of 1.2 or 1.8 c/c the translocated content of a single cell resides predominantly within one cell but for a velocity of 1.5 c/c the material is evenly distributed between two cells. This artifactual dispersion was not observed in the prototype algorithm described previously (Stevens & Schiffer, 1981) as a result of the restriction of velocity parameters to integral values. Although numerical dispersion exists in the present algorithm, it does not appear to introduce a serious problem in the context of the current experiments. The short run times used to collect the data reported here provided for significant chromatographic dispersion but little diffusion. As a result, the band spreading obtained in the simulated chromatograms is effectively the spreading due to the numerical dispersion supplemented by the spreading obtained by the Gaussian dispersion term used in the translocation routine. Because the value of the Gaussian dispersion term is estimated by direct comparison of simulated and experimental data, the consequences of the existence of numerical dispersion are minimal at current flow rates. However, for anticipated experimental strategies utilizing lower flow rates, a more detailed analysis of dispersion and diffusion parameters is under way. The problem of the numerical artifact can be minimized in practice by adoption of the strategy of Dishon et al. (1966), in which the cell size is smaller early in the simulated run.

Experimental Setup. The experimental aspects of small-zone exclusion chromatography for protein interaction study do not critically depend on any of the specific features we have incorporated into the system used for data acquisition. Computer control of the chromatography process is not an experimental prerequisite, and any appropriate pump, column,

and resin configuration may be used. However, interpretation of results is dependent upon comparison of three chromatograms, the two components run individually and the run of the mixture. Therefore, chromatography hardware optimized for reproducibility is a factor in quantitative studies based on this methodology. Choice of appropriate resin is determined by suitable resolution features and absence of interfering interactions with the reactants (Short et al., 1985). Interfering interactions will result in unpredictable elution characteristics of the complex. Because the average surface properties of the complex are not necessarily the same as the average surface properties of the components, the complex may interact differently with the chromatography matrix. In fact, the existence of these differences in surface properties is the basis of countercurrent procedures to evaluate protein–protein interaction (Backman, 1982). We have found the agarose-based (Hagel & Andersson, 1984) Superose medium to perform satisfactorily in the presence of 0.15 M NaCl for the current experiments. Rigidity of the 10-μm particles has provided tolerance of high linear flow rates while contributing sufficient resolution for our purposes in the microbore column configuration.

Binding Constant of Rheumatoid Factor SCH. The observations summarized above in Figure 8 and Table I lead to the conclusion that the SCH Fab and the DRI Fc interaction is characterized by the ability of the Fc to bind two molecules of Fab. This observation is consistent with the symmetric conformation of IgG Fc, composed of the C_{γ_2} and C_{γ_3} domains of two identical heavy chains (Nisonoff et al., 1975). However, the functional valence of the Fc relative to that of an RF has remained ambiguous; studies by Abraham et al. (1972) and Stone and Metzger (1968) reported interactions in which the Fc component appeared univalent. Multiple binding sites exist on the Fc to which various RF molecules bind (Natvig et al., 1972). Therefore, the results described above for the SCH RF and DRI Fc do not contradict the possibility that other RF/Fc interactions may be univalent.

The estimated value of K_a for the reaction between the SCH Fab and the DRI Fc is consistent with other estimates of the strength of the RF affinity for the Fc. Stone and Metzger (1968) obtained a K_a of 1.7×10^4 M^{-1} for an IgM Fab and IgG; studies by Normansell (1970) and others (Steward et al., 1973) reported K_a values of approximately 10^5 M^{-1} for several IgM RFs with respect to binding myeloma Igs of the IgG1, IgG2, and IgG4 subclasses. Comparable values were obtained by Pope et al. (1975) in an investigation of IgG RFs. A K_a value of at least 10^6 M^{-1} was inferred in a calorimetric study (Rialdi et al., 1984) of an IgM RF; a similar affinity, 1.5×10^6 M^{-1}, was observed by Abraham et al. (1972) in a study of an IgA RF.

Usefulness of Method. Within the context of antibody–antigen studies, molecular sizes range from 150000 for an IgG to approximately 14000 for a single domain subunit. The sedimentation coefficients obtained by Calvanico and Tomasi (1971) ranged from 6.8 to as low as 2.1 for these molecules. Hence, diffusion can be expected to contribute significantly to the sedimentation characteristics of these fragments and their complexes. A collection of different antibodies against the same epitope will be expected to exhibit a wide range of K_a values and possess significant heterogeneity of binding site composition. Ability to utilize a single methodology in comparative studies will contribute to minimizing ambiguity that may be introduced by different characteristic systematic errors inherent in different techniques. Further refinement of procedures allowing analysis of the delta is expected to enable interaction studies of heterogeneous preparations, including evaluations of partially purified reagents. In addition, analysis of the delta should allow quantification of the dependence of interactions in the presence of other macromolecules to compare functionality in physiological-like conditions to that exhibited in dilute solution.

Development of a suitable method for quantitative interpretation of protein interaction by small-zone gel chromatography can make available several features that would complement established interaction study methods. We expect small-zone chromatography to be a reagent-conservative procedure that will be of particular use in studies comparing a family of similar proteins. The current small-zone chromatography system is capable of readily visualizing samples of less than 300 ng of protein (data not shown). Utilization of 214-nm absorbance and application of numerical smoothing protocols to the microcomputer-collected digital data are expected to provide sensitivity sufficient to observe samples of 10 ng and, thus, allow quantitative studies of interactions with affinity on the order of 10^{10} M^{-1}. The ability to use the smallest possible sample to visualize interaction will also facilitate the study of irreplaceable proteins of clinical origin, such as myeloma and RF antibodies.

Acknowledgments

I extend sincere appreciation to Clint Ainsworth whose excellent experimental technique provided high-quality chromatographic data, to William Eisler and Don LeBuis for their contributions to the assembly of the microcomputer interface and data acquisition systems, to Frank Williamson and Carol Fox for assistance in developing the analytical and data management software, and to Drs. Marianne Schiffer and W. Carey Hanly for critical discussions. This paper is dedicated to the memory of Mrs. Gloria Zolkiewicz.

References

Abraham, G. N., Clark, R. A., & Vaughn, J. H. (1972) *Immunochemistry 9*, 301–315.

Ackers, G. K. (1975) *Proteins (3rd Ed.) 1*, 1–94.

Ackers, G. K., & Thompson, T. E. (1965) *Proc. Natl. Acad. Sci. U.S.A. 53*, 342–349.

Andrews, P. (1964) *Biochem. J. 91*, 222–233.

Backman, L. (1982) *J. Chromatogr. 237*, 185–198.

Calvanico, N. J., & Tomasi, T. B. (1971) *Arch. Biochem. Biophys. 144*, 269–280.

Cann, J. R. (1982) *Mol. Immunol. 19*, 505–514.

Cann, J. R., & Goad, W. B. (1965) *J. Biol. Chem. 240*, 148–155.

Cann, J. R., & Hinman, N. D. (1976) *Biochemistry 15*, 4614–4622.

Cox, D. J. (1965a) *Arch. Biochem. Biophys. 112*, 249–258.

Cox, D. J. (1965b) *Arch. Biochem. Biophys. 112*, 259–266.

Cox, D. J. (1969) *Arch. Biochem. Biophys. 129*, 106–123.

Cox, D. J. (1978) *Methods Enzymol. 48*, 212–242.

Cox, D. J., & Dale, R. S. (1981) in *Protein-Protein Interactions* (Frieden, C., & Nichol, L. W., Eds.) pp 173–211, Wiley, New York.

Dickerman, J., Clevinger, B., & Friedenson, B. (1981) *J. Exp. Med. 151*, 1275–1285.

Dishon, M., Weiss, G. H., & Yphantis, D. A. (1966) *Biopolymers 4*, 449–455.

Endo, S., & Wada, A. (1983) *Biophys. Chem. 18*, 291–301.

Endo, S., Hayashi, H., & Wada, A. (1982) *Anal. Biochem. 124*, 372–379.

Gilbert, G. A., & Jenkins, R. C. (1959) *Proc. R. Soc. London, Ser. A 253*, 420–437.

Gilbert, L. M., & Gilbert, G. A. (1978) *Methods Enzymol. 48*, 195–212.
Hagel, L., & Andersson, T. (1984) *J. Chromatogr. 285*, 295–306.
Hummel, J. P., & Dreyer, W. J. (1962) *Biochim. Biophys. Acta 63*, 530–532.
Kegeles, G., & Cann, J. R. (1978) *Methods Enzymol. 48*, 248–270.
Kosaka, M., & Solomon, A. (1980) *Am. J. Med. 69*, 145–154.
Maeda, H., Steffen, E., & Engel, J. (1978) *Biophys. Chem. 9*, 57–64.
Natvig, J. B., Gaarder, P. I., & Turner, M. W. (1972) *Clin. Exp. Immunol. 12*, 177–184.
Nichol, L. W., & Ogston, A. G. (1965) *Proc. R. Soc. London, Ser. B 163*, 343–368.
Nisonoff, A., Hopper, J. E., & Spring, S. B. (1975) *The Antibody Molecule*, Academic Press, New York.
Normansell, D. E. (1970) *Immunochemistry 7*, 787–797.
Plaut, A. G., Gilbert, J. V., & Wistar, R. (1977) *Infect. Immun. 17*, 130–135.
Pope, R. M., Teller, D. C., & Mannik, M. (1975) *J. Immunol. 115*, 365–373.
Rialdi, G., Raffanti, S., & Manca, F. (1984) *Mol. Immunol. 21*, 945–948.
Short, M. T., Westholm, F. A., Schiffer, M., & Stevens, F. J. (1985) *J. Chromatogr. 323*, 418–423.
Stevens, F. J., & Schiffer, M. (1981) *Biochem. J. 195*, 213–219.
Stevens, F. J., & Ainsworth, C. F. (1985) *Fed. Proc., Fed. Am. Soc. Exp. Biol. 44*, 1077.
Stevens, F. J., Westholm, F. A., Solomon, A., & Schiffer, M. (1980) *Proc. Natl. Acad. Sci. U.S.A. 77*, 1144–1148.
Steward, M. W., Turner, M. W., Natvig, J. B., & Gaarder, P. I. (1973) *Clin. Exp. Immunol. 15*, 145–152.
Stone, M. J., & Metzger, H. (1968) *J. Biol. Chem. 243*, 5977–5984.
Sullivan, B., & Riggs, A. (1967) *Biochim. Biophys. Acta 140*, 274–283.
Van Holde, K. E. (1975) *Proteins (3rd Ed.) 1*, 225–291.
Winzor, D. J., & Scheraga, H. A. (1963) *Biochemistry 2*, 1263–1267.
Wittner, M. K., Bach, M. A., & Kohler, H. (1982) *J. Immunol. 128*, 595–599.
Zimmerman, J. K. (1974) *Biochemistry 13*, 384–389.
Zimmerman, J. K., & Ackers, G. K. (1971) *J. Biol. Chem. 246*, 7289–7292.
Zimmerman, J. K., Cox, D. J., & Ackers, G. K. (1971) *J. Biol. Chem. 246*, 4242–4250.

Multiplicity of Glutathione *S*-Transferase Genes in the Rat and Association with a Type 2 Alu Repetitive Element

Gail S. Rothkopf, Claudia A. Telakowski-Hopkins, Ronald L. Stotish, and Cecil B. Pickett*

Department of Molecular Pharmacology and Biochemistry, Merck Sharp & Dohme Research Laboratories, Rahway, New Jersey 07065

Received August 23, 1985

ABSTRACT: Southern blot analysis of rat genomic DNA using glutathione *S*-transferase Ya and Yc cDNA probes was employed to estimate the size of the Ya/Yc multigene family. A minimum of five to seven Ya/Yc genes were detected; at least two of these are Yc genes. The presence of multiple genes was further supported by the isolation of three nonoverlapping genomic clones from a rat *Eco*RI library that hybridized to a Ya cDNA clone, pGTB38. However, not all *Eco*RI bands seen in genomic blots were represented in the clones, suggesting that not all Ya/Yc genes have been isolated. The organization of a Ya gene in one of these *Eco*RI genomic clones, λGTB38-3, and an overlapping clone, λGTB45-1, isolated from a *Hae*III library, was investigated with 5′ and 3′ probes prepared from Ya and Yc cDNA clones. Restriction endonuclease mapping and hybridization studies revealed that the gene spans over 10 kilobases and contains at least three introns. Sequences upstream from the 5′ untranslated region of the gene, and within an intron in the 5′ coding region, were found to contain sequences homologous to a type 2 Alu repetitive element from the rat growth hormone gene [Page, G. S., Smith, S., & Goodman, H. M. (1981) *Nucleic Acids Res. 9*, 2087–2104]. The repetitive sequences in λGTB38-3 were identified by hybridization to a novel Ya cDNA clone, pGTB45. This cDNA clone was isolated from a cDNA library previously described [Telakowski-Hopkins, C. A., Rodkey, J. A., Bennett, C. D., Lu, A. Y. H., & Pickett, C. B. (1985) *J. Biol. Chem. 260*, 5820–5825] with nick-translated intron sequences as probes. pGTB45 is virtually identical with pGTR261 [Tu, C.-P. D., Lai, H.-C. J., Li, N.-Q., Weiss, M. J., & Reddy, C. C. (1984) *J. Biol. Chem. 259*, 9434–9439], except that the 3′ untranslated region extends 231 base pairs beyond the polyadenylation signal of pGTR261. This elongated 3′ untranslated sequence is unique in that it contains a full-length type 2 Alu repetitive element, which includes two additional, overlapping polyadenylation signals.

The glutathione *S*-transferases catalyze the conjugation of the reduced sulfhydryl group of glutathione with electrophilic centers (Jacoby, 1978). Reactive groups of toxic xenobiotic compounds and potentially toxic endogenous metabolic intermediates (Meyer & Ketterer, 1982) are blocked, thus precluding attack on sensitive macromolecules such as protein

* Address correspondence to this author.

0006-2960/86/0425-0993$01.50/0